HOKKAIDO UNIVERSITY

Title	PIPKs are essential for rhizoid elongation and caulonemal cell development in the moss Physcomitrella patens
Author(s)	Saavedra, Laura; Balbi, Virginia; Lerche, Jennifer; Mikami, Koji; Heilmann, Ingo; Sommarin, Marianne
Citation	The plant journal, 67(4), 635-647 https://doi.org/10.1111/j.1365-313X.2011.04623.x
Issue Date	2011-08
Doc URL	http://hdl.handle.net/2115/49917
Rights	The definitive version is available at www.blackwell-synergy.com
Type	article (author version)
File Information	Physiological role of PpPIPKs_resubmission_2LS.pdf

Instructions for use

Full title:

PIPKs are essential for rhizoid elongation and caulonemal cell development in the moss

Physcomitrella patens

Authors:

Laura Saavedra[1,2*], Virginia Balbi[1], Jennifer Lerche[4,5], Koji Mikami[3], Ingo Heilmann[4,5],

and Marianne Sommarin[2]

Institutions:

[1]Department of Biochemistry, Center for Chemistry and Chemical Engineering, Lund
University, PO Box 124, SE-22100 Lund, Sweden

[2]Department of Plant Physiology, Umeå Plant Science Centre, Umeå University, SE-90187,
Umeå, Sweden

[3]Faculty of Fisheries Sciences (K.M.), Hokkaido University, Hakodate 041–8611, Japan

[4]Department of Plant Biochemistry, Albrecht-von-Haller-Institute for Plant Sciences,
Georg-August-University Göttingen, 37077 Göttingen, Germany

[5]New address: Department of Cellular Biochemistry, Institute for Biochemistry and
Biotechnology, Martin-Luther-University Halle-Wittenberg, 06108 Halle (Saale), Germany

* Correspondence author: Laura Saavedra; Current address: Universidade de Lisboa,
Faculdade de Ciencias de Lisboa, BioFIG, 1749-016, Lisboa, Portugal. E-mail:
llborelli@fc.ul.pt

E-mail addresses:

Laura Saavedra: llborelli@fc.ul.pt

Virginia Balbi: from.virginia@gmail.com

Jennifer Lerche: jennifer.lerche@biochemtech.uni-halle.de

Ingo Heilmann: ingo.heilmann@biochemtech.uni-halle.de

Koji Mikami: komikami@fish.hokudai.ac.jp

Marianne Sommarin: marianne.sommarin@plantphys.umu.se

Word count: 6838

SUMMARY

PtdIns-4,5-bisphosphate is a lipid messenger of eukaryotic cells playing critical roles in processes such as cytoskeleton organization, intracellular vesicular trafficking, secretion, cell motility, regulation of ion channels and nuclear signalling pathways. The enzymes responsible for the synthesis of PtdIns(4,5)P_2 are phosphatidylinositol phosphate kinases (PIPKs). The moss *Physcomitrella patens* contains two PIPKs, PpPIPK1 and PpPIPK2. To study their physiological role, both genes were disrupted by targeted homologous recombination and as a result mutant plants with lower PtdIns(4,5)P_2 levels were obtained. A strong phenotype for *pipk1*, but not for *pipk2* single knockout lines, was obtained. The *pipk1* knockout lines were impaired in rhizoid and caulonemal cell elongation, whereas *pipk1-2* double knockout lines showed dramatic defects in protonemal and gametophore morphology manifested by the absence of rapidly elongating caulonemal cells in the protonemal tissue, leafy gametophores with very short rhizoids, and loss of sporophyte production. *pipk1* complemented by overexpression of *PpPIPK1* fully restored the wild type phenotype whereas overexpression of the inactive PpPIPK1E885A did not. Overexpression of *PpPIPK2* in the *pipk1-2* double knockout did not restore the wild type phenotype demonstrating that *PpPIPK1* and *PpPIPK2* are not functionally redundant. In vivo imaging of the cytoskeleton network revealed that the shortened caulonemal cells in the *pipk1* mutants was the result of the absence of the apicobasal gradient of cortical F-actin cables normally observed in wild type caulonemal cells. Our data indicate that both PpPIPKs play a crucial role in the development of the moss *P. patens*, and particularly in the regulation of tip growth.

INTRODUCTION

Phosphoinositides (PIs) are membrane phospholipids with important regulatory and signalling roles in eukaryotic cells. Phosphatidylinositol-4,5-bisphosphate [PtdIns(4,5)P_2] is the immediate precursor of the pivotal second messengers, diacylglycerol [DAG] and inositol-1,4,5-trisphosphate [Ins(1,4,5)P_3] (Berridge, 1983; Hinchliffe and Irvine, 1997). As a messenger molecule by itself, PtdIns(4,5)P_2 plays critical roles in cytoskeleton organization, intracellular vesicular trafficking, secretion, cell motility, regulation of ion channels and nuclear signalling pathways in various eukaryotic models (Heck *et al.*, 2007). Despite of several recent reports from the plant field, knowledge on PtdIns(4,5)P_2 functions in plants is still limited (Thole and Nielsen, 2008; Heilmann, 2009). The synthesis of PtdIns(4,5)P_2 is catalyzed by PtdIns$P$ kinases (PIPKs). The basic structure shared by animal, yeast and plant PIPKs consists of a highly conserved central kinase domain and a dimerization domain (Mueller-Roeber and Pical, 2002). In addition, most plant PIPKs contain a unique conserved domain at the N terminus, the MORN domain (Membrane Occupation and Recognition Nexus) characterized by repetitions of MORN motifs (Mueller-Roeber and Pical, 2002). For instance, the *A. thaliana* genome contains eleven genes encoding type I/II A and B PIPKs. Subfamily A consists of two members, AtPIPK10 and AtPIPK11, which lack the MORN domain at the N terminus and exhibit a domain structure similar to human type I PIPKs, whereas the other nine isoforms in subfamily B contain the N-terminal MORN domain (Mueller-Roeber and Pical, 2002).

In flowering plants, PtdIns(4,5)P_2 was shown to be localized at the tip of pollen tubes (Kost *et al.*, 1999; Ischebeck *et al.*, 2008; Sousa *et al.*, 2008) and root hairs (Braun *et*

4

al., 1999; Vincent *et al.*, 2005; Kusano *et al.*, 2008; Stenzel *et al.*, 2008; Ischebeck *et al.*, 2010) leading to the suggestion that PtdIns(4,5)P_2 plays a role in the regulation of directional tip growth of plant cells. Tip growth involves signalling components from multiple pathways, such as Ca^{2+}, protein kinases, cAMP, Ras-like small GTPases, phosphoinositides, targeted vesicle fusion, and specific cytoskeleton arrangements (Hepler et al., 2001; Cole and Fowler, 2006; Malhó, 2006). Until now, only a few studies have dealt with the physiological roles of plant PIPKs. Lack of PIPKs has been shown to affect tip growth and sugar signalling in *A. thaliana* roots, and floral initiation in rice (Kusano *et al.*, 2008; Stenzel *et al.*, 2008). In *A. thaliana*, it was shown that root hair development requires AtPIP5K3-dependent PtdIns(4,5)P_2 production in the apical region of root hair cells (Kusano *et al.*, 2008; Stenzel *et al.*, 2008). *AtPIPK4* and *AtPIPK5* are pollen-specific isoforms, and pollen of T-DNA insertion lines deficient in both enzymes exhibited reduced pollen germination and defects in pollen tube elongation (Ischebeck *et al.*, 2008; Sousa *et al.*, 2008) which were associated with a reduction in endocytosis and membrane recycling in the mutant pollen tubes. Moreover, excessive PtdIns(4,5)P_2 production by these lipid kinases disturbs the balance of membrane trafficking and apical pectin deposition (Ischebeck *et al.*, 2008). Other pollen-specific isoforms, PIP5K10 and PIP5K11, are important for pollen tube polarity. However, the mechanisms of action of PtdIns(4,5)P_2 produced by these subfamily A PIPKs appears to differ from that reported previously (Ischebeck *et al.*, 2008; Sousa *et al.*, 2008) in that membrane trafficking and secretion are not affected, but rather the actin cytoskeleton (Ischebeck *et al.*, 2010). Additionally, *AtPIP5K9* was shown to interact with the cytosolic invertase CINV1 to negatively regulate sugar-mediated root cell elongation (Lou *et al.*, 2007) . In rice, OsPIPK1 is involved in

5

shoot growth and floral initiation through the regulation of floral induction genes (Ma *et al.*, 2004). The reports of PtdIns(4,5)P_2 effects in both monocot and dicot plants suggests that PtdIns(4,5)P_2 functions have been evolutionarily conserved.

The last common ancestor of the moss, *Physcomitrella patens*, and higher land plants dates back more than an estimated 400 million years (Rensing *et al.*, 2008), providing a view on the evolutionary history of PIPKs. *P. patens* has two PIPK genes, *PpPIPK1* and *PpPIPK2,* which belong to the type I/II B subfamily (Ischebeck *et al.*). In vitro, the corresponding enzymes are able to synthesize PtdIns(4,5)P_2, PpPIPK1 being the more active enzyme (Saavedra *et al.*, 2009). *P. patens* has emerged as a powerful model system for studying plant functional genomics because of its high frequency of homologous recombination (Schaefer and Zryd, 1997). The *P. patens* life cycle is dominated by a photoautotrophic haploid gametophytic generation that supports a relatively simple and mainly heterotrophic diploid sporophyte generation. The haploid gametophyte is characterized by two distinct developmental stages, the protonema and the gametophore or leafy shoot. The protonema consists of a filamentous network of chloronemal and caulonemal cells, which develop by apical growth and cell division of apical and subapical cells. The gametophore differentiates by caulinary growth from a simple apical meristem, the bud. The gametophore is made up of a photosynthetic non-vascularized stem, which carries the leaves, the reproductive organs and the filamentous rhizoids that arise from the base of the stem (Schaefer and Zryd, 2001).

This study addresses the physiological role of PIPKs in *P. patens* through the targeted disruption of *PpPIPK1* and *PpPIPK2* by homologous recombination. We show that double knockout *pipk1-2* lines show a dramatic phenotype with defects in protonemal

and gametophore morphology manifested as lack of the rapidly elongating caulonemal cell type in the protonemal tissue, leafy gametophores with very short rhizoids, and loss of sporophyte production. Use of an inducible GFP-talin to detect the actin cytoskeleton in living tissue (Finka *et al.*, 2007) revealed that the reduced elongation of the caulonemal cells observed in the *pipk1* knockout line was correlated with the absence of the apico-basal gradient distribution of the F-actin meshwork characteristic of wild type caulonemal cells. Taken together, our results indicate that the moss PIPKs are involved in tip growth by affecting the F-actin cytoskeleton network.

RESULTS

PpPIPK1 and *PpPIPK2* affect rhizoid and caulonemal cell elongation

The two moss PIPKs, PpPIPK1 and PpPIPK2, exhibit high sequence similarity at the gene and protein levels, however, the recombinant enzymes differed with respect to specific activities and substrate specificity (Saavedra *et al.*, 2009). To further dissect the role of these two enzymes in *P. patens*, we generated *pipk* null mutants by homologous recombination using targeted gene disruption (Suppl. Figure 1A and Table I). For the generation of *pipk1-2* double knockouts, *pipk1* and *pipk2* single knockout lines were transformed with a *PIPK2* or a *PIPK1* deletion construct, respectively. After antibiotic selection, targeted disruption events were detected by simultaneous PCR amplifications using gene-specific primers external to the targeting construct in combination with outward-oriented primers specific to the selectable marker cassette (Suppl. Figure 1A and Table I). For the *pipk1* knockout lines, a PCR product of 2468 bp and 1445 bp for the left

and right borders, respectively should be amplified, whereas for the *pipk2* knockout lines, PCR fragments of 2379 bp and 1379 bp should be amplified for left and right borders, respectively (Suppl. Figure 1B). PCR products of the expected sizes were obtained. Positive transformants analyzed by PCR were selected and the transcript pattern was analyzed by RT-PCR with specific primers (Table I). In the wild type, transcripts of 918 bp and 919 bp for *PIPK1* and *PIPK2*, respectively, were amplified; whereas the mutants completely lacked the respective transcripts (Suppl. Figure 1C). Two lines for each of the *pipk1* (#5 and #8), *pipk2* (#2 and #27) and *pipk1-2* (#38 and #6) knockouts giving stable phenotypes were isolated from independent transformations and used for detailed analyses.

The phenotypes of the wild type and the *pipk* knockout lines during different developmental stages of *P. patens* life cycle are shown in Figure 1 (A-E). Colony morphology of *pipk1* knockout lines showed a dramatic reduction of protonema and rhizoid growth compared to wild type (Figure 1 A-B). The *pipk1* knockout leafy gametophores developed earlier than in the wild type (data not shown). As seen in Figure 1C *pipk1* knockout protonemata appeared more green than the wild type and showed a reduction in individual cell length. The *pipk1* knockout lines were able to complete the life cycle and produce normal sporophytes (Figure 1 D-E). The phenotype of the single *pipk2* mutant did not differ significantly from the wild type (Figure 1 A-E). Importantly, *pipk1-2* double knockout lines showed a more pronounced phenotype compared to the single *pipk1* knockout lines. Protonemal filaments exhibited a compact structure, and were composed of shorter cells. The double knockout showed a distinct delay in the gametophore development, as well as very short rhizoids. Importantly, the double knockout did not produce sporophytes (Figure 1 A-E).

To further characterize the transformant phenotype some morphometric parameters (Vidali *et al.*, 2007) were evaluated (Figure 1F). Colony total area was similar for the wild type and for *pipk2* knockout lines whereas a reduction in size of 84 and 89% was observed for *pipk1* and *pipk1-2* knockout lines, respectively. Solidity is defined as area/convex hull area, and plants with values approaching one are more compact. Solidity values were close to 1 in *pipk1* and *pipk1-2* knockout lines, which agrees with the observed reduction in protonemal filament extension whereas *pipk2* knockout and wild type exhibited average values of 0.2 (Figure 1F).

The levels of regulatory phospholipids are altered in the *pipk* mutants

In order to test the effects of the knockouts on the endogenous phospholipid levels; PtdIns(4,5)P_2, PtdIns (phosphatidylinositol) and PtdCho (phosphatidylcholine) were quantified in the wild type and *pipk* knockout lines using moss protonema under normal growth conditions (Figure 2). While the levels of the structural phospholipid, PtdCho, showed no significant difference between the wild type and the *pipk* knockout lines, a reduction of PtdIns(4,5)P_2 content was obvious in both the single *pipk* knockouts and in the *pipk1-2* double knockout lines when compared to the wild type. Interestingly, the levels of PtdIns-monophosphates, representing the sum of PtdIns3P and PtdIns4P, were not significantly changed (data not shown). PtdIns levels were slightly increased in the knockout lines over the wild type controls. The data indicate that the lack of the respective *PIPK* gene in the transformants can be attributed to differences in PtdIns(4,5)P_2 content, because other phospholipids were not significantly affected in the knockout lines. Importantly, the data show that the levels of PtdIns(4,5)P_2 were reduced in the *pipk2* single

knockout, even though no phenotypic effect was observed for this line. The data further suggest that PIPK2 and its lipid product have little effect on protonemal growth of *P. patens*.

Whereas wild type and *pipk2* knockout lines have similar chlorophyll content, *pipk1* and *pipk1-2* knockout lines have double the amount of chlorophyll a + b, thus explaining their greener phenotype (Figure 3A). To distinguish between chloronemal and caulonemal cells we used Calcofluor staining, which binds to and visualizes the cell wall. Chloronemal cells contain cell walls that are perpendicular to the filament axis while caulonemal cell walls are oblique to the filament axis. When grown in minimal media, *pipk1* and *pipk2* knockout lines exhibited chloronemal cell lengths with average values similar to wild type, 100 μm (Figure 3B). Average caulonemal cell length in wild type and *pipk2* knockout was 200 μm, whereas the corresponding cells in *pipk1* knockout were only half this length (Figure 3B). It was not possible to identify typical caulonemal cells in the *pipk1-2* double knockout lines; in these mutants the protonema consists of short cells with an average length of 70 μm (Figure 3B).

It is commonly accepted that only caulonemal cells, which constitute the adventitious part of the protonema, are responsible of producing buds (Schumaker and Dietrich, 1997). To verify the observed lack of caulonemal cells in the *pipk1-2* double knockout lines we utilized the ability of caulonemal, but not chloronemal cells, to grow in the dark (Cove *et al.*, 1978). Figure 3C shows moss lines grown in the dark for 20 days. Plates were grown upright to aid visualization because in the absence of light *P. patens* filaments will orient their growth with respect to gravity (Jenkins and Cove, 1983). Wild

10

type and *pipk2* knockout lines showed substantial growth in the dark, while a strong reduction in caulonemal cell growth was observed for *pipk1* knockout lines (Figure 3C). No detectable growth was observed in *pipk1-2* double knockout lines (Figure 3C), confirming the absence of the typical caulonemal cell type.

In addition to defects in caulonema development, rhizoid development was also altered in the mutant lines. It is important to note that rhizoids are multicellular filamentous structures, which resemble caulonemal filaments. They differentiate from the bottom part of the bud and function in the attachment of leafy shoots to the substratum and in the uptake of nutrients. Rhizoids that developed from the *pipk1* and *pipk1-2* knockout gametophores showed strong defects in cell elongation with average length values of 0.38 cm for wild type and *pipk2*, and 0.060 cm and 0.037 cm for *pipk1* and *pipk1-2* knockout lines, respectively (Figure 4A-B).

Thus, the impaired growth phenotype exhibited by *pipk1* and *pipk1-2* knockout mutants could be explained by defects in the development of caulonemal cells as well as in rhizoid development. Interestingly, whereas in wild type bud differentiation occurs in caulonema cells, in the *pipk1-2* double knockout mutants buds differentiated from chloronema cells. Additionaly, *pipk1-2* double knockout lines were not able to produce sporophytes.

P. patens **wild type treated with cytochalasin B mimics the** *pipk1* **knockout phenotype**

PtdIns(4,5)P_2 is involved in the regulation of the cytoskeleton organization. To determine if the disruption of the *PpPIPK* genes affects the actin cytoskeleton, we looked at the effect of cytochalasin B (Cyt B), a specific and efficient F-actin drug, that inhibits rapid

cell elongation in plants (Thimann *et al.*, 1992). Cyt B binds to the barbed ends of actin filaments (AFs), which then do not grow further and consequently depolymerise due to the inherent loss of monomers at their pointed ends (Cooper, 1987). When wild type protonema was grown in minimal media with the addition of 10 µM Cyt B, filament growth by cell extension was dramatically affected and the phenotype observed closely resembled the *pipk1* knockout phenotype without drug treatment (Figure 5A). Cyt B-treated *pipk2* knockout lines exhibited the same phenotype as wild type controls, whereas the addition of Cyt B to *pipk1* knockout lines further strengthened the inhibition of the protonemal cell elongation. However, no effect was observed in Cyt B-treated *pipk1-2* double knockout lines. DMSO treatment of all *pipk* knockout lines or wild type controls did not significantly affect protonemal growth compared to growth in minimal media (Figure 5A).

Latrunculin B (Lat B) is another F-actin-destabilizing drug, which causes a shift from F-actin to G-actin. Since the process of protoplast regeneration mimics spore germination and it is possible to follow the establishment of cell polarity, the effect of Cyt B and Lat B was tested on wild type and *pipk* protoplasts. Two-day-old protoplasts of wild type and mutants were transferred to a media containing either 10 µM Cyt B or 5 µM Lat B and analyzed 3 days after drug treatment (Figure 5B). For wild type and *pipk2* knockout lines normal growth and establishment of polarity was observed under control conditions, whereas a pronounced reduction in cell elongation was observed upon treatments with Cyt B or Lat B. Wild type lines growing in the presence of Cyt B showed the same phenotype as *pipk1* knockout lines growing in control (DMSO) media. However, the *pipk1* knockout lines were affected by Cyt B and Lat B, displaying an even stronger phenotype under these

conditions. A general observation was that the treatment with Lat B affected growth more dramatically than Cyt B. Interestingly, the *pipk1-2* double mutants showed a strong defect in the establishment of polar growth after 5 days; cells were more circular and no significant difference between DMSO and Cyt B or Lat B treatments was observed.

PpPIPK1 but not *PpPIPK1E885A* restored the wild type phenotype

To test the specificity of the *pipk1* knockout phenotype, *pipk1* knockout protoplasts were transformed with a *PpPIPK1* overexpression construct driven by the maize ubiquitin promoter (Anterola *et al.*, 2009), a hygromycin resistance cassette and a fragment of the 108 genomic loci as targeting sequence. PpPIPK1 overexpression complemented the *pipk1* knockout phenotype (Figure 6 A). The *pipk*1 knockout plus *PpPIPK1* phenotype resulted in normal rhizoid elongation and protonemal growth with, chloronemal and caulonemal cell types, as well as restoration of caulonema cell elongation. These results demonstrate that the mutant phenotype observed in *pipk1* knockout lines was truly a result of the *PIPK1* disruption. In previous experiments (Saavedra *et al.*, 2009) we have shown that PpPIPK1 activity is almost completely abolished towards PtdIns4*P* by altering the glutamic acid residue at position 885 to alanine. When *pipk1* knockout protoplasts were transformed with *PpPIPK1E885A*, the resulting line did not show the wild type phenotype (Figure 6 A). Values for rhizoid and caulonemal cell lengths in this line were higher than in the *pipk1* mutant but not as high as in wild type controls (Figure 6 C-D). The data confirm that the glutamic acid at position 885 is essential for the activity of PpPIPK1 in vivo.

Overexpression of *PpPIPK2* in the *pipk1-2* double knockout did not restore the wild type phenotype

Since the *pipk2* single mutant did not differ significantly from the wild type phenotype, we used the *pipk1-2* double mutant to test the addition of *PpPIPK2*. Interestingly, the *pipk1-2* plus *PpPIPK2* mutant showed a phenotype similar to the single *pipk1* knockout mutant, with caulonemal cell and rhizoid development restored to *pipk1* single knockout levels (Figure 6 A-D).

The actin organization in *pipk1* knockout caulonemal cells is affected

Because the phenotype resulting from treatment of *P. patens* wild type controls with Cyt B resembled that of the untreated *pipk1* mutant, we investigated the actin cytoskeleton in the knockout and wild type lines. For the in vivo visualization of F-actin, the *P. patens* line *hgt-1* was used, which expresses GFP-talin under a soybean heat-inducible promoter (Finka *et al.*, 2007). *pipk1* and *pipk2* single knockout lines were generated in the *P. patens hgt-1* background (Supplemental Figure 2) and the actin cytoskeleton was observed using confocal laser scanning microscopy (CLSM). For these studies, protonemal tissues of *hgt-1* controls, *pipk1* knockout (*hgt-1*) and *pipk2* knockout (*hgt-1*) were grown in minimal media and heat shocked for 1 h at 37 °C. GFP-talin was observed 12 h after induction. As shown in Supplemental Figure 3 apical chloronemal cells of *hgt-1*, the *pipk1* knockout (*hgt-1*) and the *pipk2* knockout (*hgt-1*) did not show significant differences in the F-actin distribution and accumulation in chloronemal cells. The patterns observed resembled those previously described for the *hgt-1* strain (Finka *et al.*, 2007) where F-actin accumulates at the tip and is connected to a cortical F-actin network along the cell. Wild type controls and single

knockout lines also showed a similar pattern characterized by caps of F-actin at new side branches (data not shown). In wild type *hgt-1* apical caulonemal cells, accumulation of the F-actin cap array located either at the end of the tip or at its apical side. However, as previously reported, caulonemal cells display an apicobasal gradient of the cortical actin meshwork; a dense F-actin network close to the tip which becomes more diffuse towards the end of the cell (Figure 7A). The apicobasal gradient was observed in apical and subapical caulonemal cells of *hgt-1* controls (Figure 7 A, D) and in the *pipk2* knockout (*hgt-1*) line (Figure 7 C, F). Importantly, the pattern of the apicobasal gradient of cortical actin was altered in the *pipk1* knockout (*hgt-1*) (Figure 7 B, E). Even though apical caulonemal cells of the *pipk1* knockout (*hgt-1*) still exhibited the apical F-actin cap, the apicobasal gradient of the cortical F-actin cables was distorted, and F-actin was evenly distributed along the whole cell (Figure 7 B). The same unorganized pattern was observed in *pipk1* knockout (*hgt-1*) subapical caulonemal cells (Figure 7 E). The data indicate that the gradient-driven organization of F-actin in caulonema cells is severely distorted in the *pipk1* (*hgt-1*) knockout mutant.

DISCUSSION

Previous studies focusing on diverse isoenzymes of PIPKs have demonstrated important roles of PtdIns(4,5)P_2 in polar tip growth in higher plants (Braun *et al.*, 1999; Kost *et al.*, 1999; Ischebeck *et al.*, 2008; Kusano *et al.*, 2008; Sousa *et al.*, 2008; Stenzel *et al.*, 2008; Ischebeck *et al.*, 2010). The fact that *P. patens* has only two *PIPK* genes and that filamentous tissues of moss chloronemal and caulonemal cells expand by tip growth

(Menand *et al.*, 2007), made this organism an interesting model to reveal whether the loss of function of PIPKs affected tip growth also in lower plants.

Our results show that the disruption of the two *PIPKs*, *PpPIPK1* and *PpPIPK2,* severely affects caulonemal growth. However, no phenotypic difference was observed between the *pipk2* single knockout lines and the wild type phenotype while *pipk1* single knockout lines showed a distinct phenotype. This result was somewhat surprising since the PtdIns(4,5)P_2 levels in both single mutants were half of those found in wild type. The addition of *PpPIPK2* to the *pipk1-2* double knockout did not restore the wild type phenotype meaning that PIPK1 and PIPK2 are not functionally redundant. The phenotypes of the single and double mutants suggested that PIPK1 was predominantly more important for the maintenance of protonemal growth with only little contribution by PIPK2. While the effect on growth by eliminating PIPK2 appears small and PIPK2 might not normally function in the context of protonemal growth, it is obvious from the results on the double knockout that PIPK2 also has some capability to impact protonemal growth, at least in the metabolic situation present in the *pipk1-2* double knockout. The double knockout analysis implicates that the PtdIns(4,5)P_2 synthesized by PIPK2 is sufficient for maintaining developmental processes lost in the double knockout. The differences in phenotypes associated with the *pipk1* and *pipk2* single mutants, respectively, is consistent with the previous in vitro characterization of recombinant PpPIPK1 and PpPIPK2 which demonstrated substantial differences in specific activity and substrate preference between the two recombinant enzymes (Saavedra *et al.*, 2009). **PIPK1 preferred substrates are PtdIns4P and PtdIns3P to produce PtdIns(4,5)P_2 and PtdIns(3,4)P_2, respectively, whereas PIPK2**

preferred PtdIns as substrate for the synthesis of PtdIns3*P* and is much less active towards PtdIns4*P* and PtdIns3*P*.

Different scenarios could explain the fact that only *pipk1* single knockout plants, but not *pipk2* single knockouts, showed a distinct phenotype (Figures 1, 3 and 4). **First**, the PtdIns(4,5)P_2 molecules produced by these two enzymes have different functions. Whether this can be explained in terms of that the two plasma membrane enzymes are activated by and interact with different cellular components, are differentially expressed and located in different tissues, cells or cell parts, or a combination remains to be established. **We have earlier shown that both *PIPKs* are expressed in protonema, gametophores at similar levels. However, *PIPK1* is much more abundant than *PIPK2* in protoplasts, and additionally, the expression of *PIPK1* is strongly induced by osmostress** (Saavedra *et al.*, 2009). **Second, PIPK2 could be responsible for producing some of the PtdIns*P* substrate required by PIPK1, which would explain that the *pipk1-2* double knockout has the most severe phenotype due to the reduction in both PtdIns*P* and PtdIns*P*$_2$, and that the addition of *PIPK2* to the double knockout restore a phenotype similar to the *pipk1* single knockout.**

The strong reduction in cell elongation observed in the moss *pipk* mutants, resembles phenotypes observed in root hairs of the *A. thaliana pip5k3* knockout (Kusano et al., 2008; Stenzel et al., 2008), pollen tubes of the *pipk4 pipk5* double knockout (Sousa et al., 2008; Ischebeck et al., 2008) or those of *pip5k10 pip5k11* double knockouts (Ischebeck *et al.*, 2010). Loss of function of these genes led to phenotypes with impaired cell elongation in cell types exhibiting tip growth. The corresponding *A. thaliana* PIPKs and their product PtdIns(4,5)P_2 were both detected at the growing apex of pollen tubes (Kost *et*

al., 1999; Dowd *et al.*, 2006; Ischebeck *et al.*, 2008; Sousa *et al.*, 2008) and root hairs (Braun *et al.*, 1999; Kusano *et al.*, 2008; Stenzel *et al.*, 2008). The phenotype observed in the *P. patens pipk1* and *pipk1-2* mutants was correlated with decreased amounts of PtdIns(4,5)P_2. It has been shown that both PpPIPKs are localized to the plasma membrane when overexpressed transiently as GFP fusions in moss protoplasts (Saavedra *et al.*, 2009; Mikami *et al.*, 2010) but it still remains to be confirmed that these enzymes are localized to the tip of the moss filaments.

Data presented in this study support the notion that PtdIns(4,5)P_2 is an essential component of the machinery controlling polar tip growth. The *P. patens pipk1* and *pipk1-2* knockout phenotypes are also closely related to other *P. patens* mutants of several members of the Arp2/3 complex (a regulator of actin filament dynamics in a wide array of eukaryotic cells), which were also affected in tip growth. The *arpc1* mutant lack the caulonemal cell type, colonies lack leafy gametophores and are defective in their ability to properly establish a polarized outgrowth during regeneration from a single cell (Harries *et al.*, 2005). In addition, the *arpc4* knockout caulonemal cells and rhizoids fail to elongate (Perroud and Quatrano, 2006), whereas the *arp3a* knockout lacks the caulonemal cell type, and the mutation was associated with the absence of the F-actin star like cap arrays at the growing tip of the cells (Finka *et al.*, 2008). Our observations are also consistent with the recent report on effects of PIPK isoforms PIP5K10 and PIP5K11 on the actin-cytoskeleton of pollen tubes in Arabidopsis and *N. tabacum* (Ischebeck *et al.*, 2010).

When *PpPIPK1* was added back to the *pipk1* mutant, the wild type phenotype was restored. Interestingly, the addition of *PpPIPK1E885A* to the *pipk1* knockout background did not completely complement the mutation. We previously showed that PpPIPK1E885A

lipid kinase activity in vitro was almost completely abolished towards PtdIns4P and PtdIns3P; but resulted in some activity with PtdIns5P (Saavedra *et al.*, 2009). Our present results with PpPIPK1E885A verify that the glutamic acid residue in the activation loop is essential for PpPIPK1 kinase activity also in vivo. Interestingly, an AtPIP5K3 mutant lacking the MORN domain, and with an in vitro kinase activity similar to the full length enzyme, could not rescue root hair growth when introduced to *pip5k3* Arabidopsis mutant plants, showing that although the mutated enzyme was active in vitro it did not seem to be functional in vivo (Stenzel *et al.*, 2008). Our data indicate that the *P. patens pipk1-2* double mutant phenotype was caused by the reduced capability to form PtdIns(4,5)P_2 and not another PtdIns-bisphosphate isomer. Based on the mutant phenotypes it can also be concluded that the so far uncharacterized genes in the *P. patens* genome that encode putative PtdIns3P 5-kinases are not contributing to the formation of a pool of PtdIns-bisphosphate with roles in polar tip growth.

F-actin has previously been shown to be essential for plant cell elongation (Baluska *et al.*, 2001). PtdIns(4,5)P_2 is known to be an important regulator of several F-actin-binding proteins (Lemmon *et al.*, 2002; Yin and Janmey, 2003). Among these, profilin and the actin depolymerising factor (ADF) are critical for the dynamics and assembly state of F-actin in plant cells, playing a critical role in *A. thaliana* and *P. patens* cell elongation (Ramachandran *et al.*, 2000; Dong *et al.*, 2001; McKinney *et al.*, 2001; Vidali *et al.*, 2007; Augustine *et al.*, 2008). However, it is still unknown whether interactions between F-actin and profilin or ADF are also conserved in mosses, and if so, how PtdIns(4,5)P_2 regulates the activity of these actin binding proteins. Cytochalasins abolish tip-growth in *P. patens* (Doonan *et al.*, 1988) and it was reported that treatment of

the *hgt-1* moss line protonemal cells with Cyt B and Lat B eliminates the apical F-actin arrays and disorganizes actin network, which in turn affects cell growth (Finka *et al.*, 2007). Using the two complementary F-actin drugs, Cyt B and Lat B, we showed that depletion of actin filaments (AFs) inhibits the onset of rapid cell elongation in the protonemata filaments of wild type plants, which resembles the protonema phenotype observed in *pipk1* knockout plants (Figure 5). This result points to the absence of *pipk* genes as having a close relation with the integrity of the AFs for tip growth. The notion that the actin fine structure of polar growing cells is controlled by PtdIns(4,5)P_2 is consistent with recent findings from Arabidopsis and tobacco (Ischebeck *et al.*, 2010). However, there are some particular observations, which might be specific for the *P. patens* system. For instance, the *pipk1* mutant in the *hgt-1* background had an apical F-actin array, but the apicobasal gradient of the cortical F-actin cables normally observed in caulonemal cells was absent. This observation suggests that the gradient of the F-actin meshwork in the caulonemal cells is necessary for proper cell elongation. More studies should be done to elucidate if PtdIns(4,5)P_2 directly regulates this process and/or if the PpPIPK proteins interact with other actin binding proteins that in turn are responsible for establishing the gradient of F-actin necessary for polar tip growth.

Experimental procedures

Plant material, culture conditions and treatments

P. patens subsp. *patens* was used for all experiments described in this study. Plant cultures were grown axenically at 24°C either under continuous light or under a long-day light cycle

(16 h of light and 8 h of darkness) with a photon flux of 60 µmol m^{-2} s^{-1}. *P. patens* protonemal tissue was routinely subcultured at 7-day intervals on cellophane disks (AA packaging, Preston, UK) overlaying Petri dishes (90 mm in diameter) containing minimal medium supplemented with 5 mM (di)ammonium tartrate, 0.8% (w/v) agar (Ashton and Cove, 1977). Phenotypic analyses were completed on minimal media without addition of (di)ammonium tartrate.

Cell measurements were performed on three first subapical cells of 6-day-old protonema stained with 10 µg/mL fluorescent brightener 28 (Sigma-Aldrich). The measurements of cell length as well as area were made by ImageJ software (http://rsb.info.nih.gov/ij/).

For the dark growth experiments, 7-day-old moss protonemata were grown for one week under continuous light on solid minimal medium supplemented with ammonium-tartrate and glucose and then grown in darkness in vertically positioned Petri dishes for 3 weeks.

For gametophore induction fresh protonemata was grown in Jiffy7 pots covered by water below 1 cm, at 24°C under continuous light. After six weeks of growth, cultures were transferred to 15 °C under short day conditions (8 h light/day) for sporophyte induction.

For the determination of chlorophyll content, 20-day-old colonies grown on cellophane discs placed on minimal media were ground up in a mortle containing 1.8 ml of 80% v/v acetone, and then the homogenized plant material was filtered to remove cell debris. Total chlorophyll was calculated as chlorophyll a + chlorophyll b (mg g^{-1} fresh weight) using the formula: Chl a mg g^{-1} = [(12.7 x Abs$_{663}$) – (2.6 x Abs$_{645}$)] x mL acetone mg^{-1} fresh tissue; Chl b mg g^{-1} = [(22.9 x Abs$_{645}$) – (4.68 x Abs$_{663}$)] x mL acetone mg^{-1} fresh tissue.

Isolation of protoplasts, polyethylene glycol–mediated transformation, regeneration and antibiotic selection were performed as described previously (Schaefer & Zryd, 1997). G418

(Sigma-Aldrich), Zeocin (Invitrogen) and Hygromycin (Invitrogen) were added at 50 mg/L, 25 mg/L and 25 mg/L to the media, respectively to select for antibiotic-resistant cells.

RT-PCR

Total RNA from 6- to 7-day-old moss protonemal tissue was isolated using the RNeasy Plant Mini Kit (Qiagen, Hilden, Germany). One microgram of total RNA was treated with one unit of DNase I (Promega) and then used as template for reverse transcription (ThermoscriptRT from Invitrogen) and primed with an oligo(dT) primer. A 1/50 volume of the cDNA was subsequently used as template for PCR. Primers used for amplification are listed in Table 1.

Generation of targeting constructs

Genomic *PpPIPK1* and *PpPIPK2* were amplified from genomic DNA with primers designed to the 5' and 3' ends of the cDNA sequence (Table 1). As target sequences for homologous recombination for gene disruption, two adjacent DNA fragments encompassing, respectively, the 5´ and 3´ regions of the *PpPIPK1* and *PpPIPK2* genes were cloned into the pUBW302 or p35S-Zeo vectors respectively, after their amplification from genomic DNA by PCR using the primer pairs (see table 1). The *PIPK1* knockout construction contained the nptII gene driven by the CaMV 35S promoter and the 3' UTR of the ocs gene, flanked by 1609 and 1045 bp of the 5' and 3' ends of the PpPIPK1 gene, respectively. For *PIPK2*, the knockout construct contained the zeo gene driven by the CaMV 35S promoter and the 3' UTR of the ocs gene, flanked by 1401 bp and 893 bp of the 5' and 3' ends of the PpPIPK2 gene, respectively. As target sequence for homologous

recombination for the complementation analysis *PpPIPK1*, *PpPIPK1A885E* or *PpPIPK2* coding sequences were amplified with specific primers (see table 1) and cloned into a pENTR/D-TOPO vector (Gateway system, Invitrogen, Sweden). The coding sequences were then cloned into the destination vector uj3 pTUbiGate (Anterola *et al.*, 2009).

Transformation of P. patens

Polyethylene glycol–mediated protoplast transformation was performed according to. In short, 6-day-old protonema were treated with 0.5% Driselase in 8.5% w/v mannitol for 30 min, passed through a 100-mm sieve, incubated for 15 min at room temperature and passed through a 50-mm sieve. The protoplasts of the final flow-through, were washed twice in 8.5% mannitol, were ready for further use. Protoplasts were transformed at a concentration of 1.6×10^6 protoplasts/mL. Each transformation consisted of 0.3 mL of protoplast suspension and 20 μg of linear DNA. To eliminate any episomal resistant colonies (Ashton et al., 2000), two rounds of selection were undertaken using the appropriate antibiotic. Transformations with complementation vectors were performed with plasmid-based vectors linearized with the appropriate restriction enzyme.

Cytochalasin B and Latrunculin B treatment

Protoplasts were prepared as described in (Schaefer and Zryd, 1997) and embedded in top-agar on cellophane disks placed on regenerating media for two days. The third day, protoplasts were transferred to the appropriate media containing either DMSO, Lat B or Cyt B. Lat B and Cyt B were prepared by diluting them to a 2 mM stock solution in DMSO. Concentrations used for physiological studies were 10 μM for Cyt B and 5 μM for Lat B.

Live Cell Microscopy and Image Analysis

For confocal microscopy, carefully excised pieces of cellophane containing undamaged five-day-old moss tissue were transferred into tubes containing 600 ml of minimal media and heat shocked twice, for 1 hour at 37 °C, with a 4 hour interval. The tissue was then placed in plates in standard growth conditions and GFP-talin was observed 12 hours after induction. Confocal microscopy was performed on a Zeiss LSM510 Meta. GFP signal was observed using an argon ion laser excitation line at 488 nm and the red (chloroplast) signal was observed using a 633 nm HeNe laser excitation line. Images were then processed using the software AxioVision Release 4.8.1 and Adobe Photoshop CS3.

Lipid analysis

Phospholipids were extracted from 250 μg of material ground in liquid nitrogen and analyzed exactly as previously described (Konig *et al.*, 2008).

REFERENCES

Anterola, A., Shanle, E., Perroud, P.F. and Quatrano, R. (2009) Production of taxa-4(5),11(12)-diene by transgenic Physcomitrella patens. *Transgenic Res*, **18**, 655-660.

Augustine, R.C., Vidali, L., Kleinman, K.P. and Bezanilla, M. (2008) Actin depolymerizing factor is essential for viability in plants, and its phosphoregulation is important for tip growth. *Plant J*, **54**, 863-875.

Baluska, F., Jasik, J., Edelmann, H.G., Salajova, T. and Volkmann, D. (2001) Latrunculin B-induced plant dwarfism: Plant cell elongation is F-actin-dependent. *Dev Biol*, **231**, 113-124.

Berridge, M.J. (1983) Rapid accumulation of inositol trisphosphate reveals that agonists hydrolyse polyphosphoinositides instead of phosphatidylinositol. *Biochem J*, **212**, 849-858.

Braun, M., Baluska, F., von Witsch, M. and Menzel, D. (1999) Redistribution of actin, profilin and phosphatidylinositol-4, 5-bisphosphate in growing and maturing root hairs. *Planta*, **209**, 435-443.

Cole, R.A. and Fowler, J.E. (2006) Polarized growth: maintaining focus on the tip. *Curr Opin Plant Biol*, **9**, 579-588.

Cooper, J.A. (1987) Effects of cytochalasin and phalloidin on actin. *J Cell Biol*, **105**, 1473-1478.

Cove, D.J., Schild, A., Ashton, N.W. and Hartmann, E. (1978) Genetic and Physiological Studies of Effect of Light on Development of Moss, Physcomitrella-Patens. *Photochemistry and Photobiology*, **27**, 249-254.

Dong, C.H., Xia, G.X., Hong, Y., Ramachandran, S., Kost, B. and Chua, N.H. (2001) ADF proteins are involved in the control of flowering and regulate F-actin organization, cell expansion, and organ growth in Arabidopsis. *Plant Cell*, **13**, 1333-1346.

Doonan, J.H., Cove, D.J. and Lloyd, C.W. (1988) Microtubules and Microfilaments in Tip Growth - Evidence That Microtubules Impose Polarity on Protonemal Growth in Physcomitrella-Patens. *Journal of Cell Science*, **89**, 533-540.

Dowd, P.E., Coursol, S., Skirpan, A.L., Kao, T.H. and Gilroy, S. (2006) Petunia phospholipase c1 is involved in pollen tube growth. *Plant Cell*, **18**, 1438-1453.

Finka, A., Schaefer, D.G., Saidi, Y., Goloubinoff, P. and Zryd, J.P. (2007) In vivo visualization of F-actin structures during the development of the moss Physcomitrella patens. *New Phytol*, **174**, 63-76.

Finka, A., Saidi, Y., Goloubinoff, P., Neuhaus, J.M., Zryd, J.P. and Schaefer, D.G. (2008) The knock-out of ARP3a gene affects F-actin cytoskeleton organization altering cellular tip growth, morphology and development in moss Physcomitrella patens. *Cell Motil Cytoskeleton*, **65**, 769-784.

Harries, P.A., Pan, A. and Quatrano, R.S. (2005) Actin-related protein2/3 complex component ARPC1 is required for proper cell morphogenesis and polarized cell growth in Physcomitrella patens. *Plant Cell*, **17**, 2327-2339.

Heck, J.N., Mellman, D.L., Ling, K., Sun, Y., Wagoner, M.P., Schill, N.J. and Anderson, R.A. (2007) A conspicuous connection: structure defines function for the phosphatidylinositol-phosphate kinase family. *Crit Rev Biochem Mol Biol*, **42**, 15-39.

Heilmann, I. (2009) Using genetic tools to understand plant phosphoinositide signalling. *Trends Plant Sci*.

Hepler, P.K., Vidali, L. and Cheung, A.Y. (2001) Polarized cell growth in higher plants. *Annu Rev Cell Dev Biol*, **17**, 159-187.

Hinchliffe, K. and Irvine, R. (1997) Inositol lipid pathways turn turtle. *Nature*, **390**, 123-124.

Ischebeck, T., Seiler, S. and Heilmann, I. At the poles across kingdoms: phosphoinositides and polar tip growth. *Protoplasma*, **240**, 13-31.

Ischebeck, T., Stenzel, I. and Heilmann, I. (2008) Type B Phosphatidylinositol-4-Phosphate 5-Kinases Mediate Arabidopsis and Nicotiana tabacum Pollen Tube Growth by Regulating Apical Pectin Secretion. *Plant Cell*, **20**, 3312-3330.

Ischebeck, T., Stenzel, I., Hempel, F., Jin, X., Mosblech, A. and Heilman, I. (2010) Phosphatidylinositol-4,5-bisphosphate influences Nt-Rac5-mediated cell expansion in pollen tubes of Nicotiana tabacum. *The Plant Journal*, **DOI: 10.1111/j.1365-313X.2010.04435.x**.

Jenkins, G.I. and Cove, D.J. (1983) Phototropism and Polarotropism of Primary Chloronemata of the Moss Physcomitrella-Patens - Responses of the Wild-Type. *Planta*, **158**, 357-364.

Konig, S., Hoffmann, M., Mosblech, A. and Heilmann, I. (2008) Determination of content and fatty acid composition of unlabeled phosphoinositide species by thin-layer chromatography and gas chromatography. *Anal Biochem*, **378**, 197-201.

Kost, B., Lemichez, E., Spielhofer, P., Hong, Y., Tolias, K., Carpenter, C. and Chua, N.H. (1999) Rac homologues and compartmentalized phosphatidylinositol 4, 5-bisphosphate act in a common pathway to regulate polar pollen tube growth. *J Cell Biol*, **145**, 317-330.

Kusano, H., Testerink, C., Vermeer, J.E., Tsuge, T., Shimada, H., Oka, A., Munnik, T. and Aoyama, T. (2008) The Arabidopsis Phosphatidylinositol Phosphate 5-Kinase PIP5K3 is a key regulator of root hair tip growth. *Plant Cell*, **20**, 367-380.

Lemmon, M.A., Ferguson, K.M. and Abrams, C.S. (2002) Pleckstrin homology domains and the cytoskeleton. *FEBS Lett*, **513**, 71-76.

Lou, Y., Gou, J.Y. and Xue, H.W. (2007) PIP5K9, an Arabidopsis phosphatidylinositol monophosphate kinase, interacts with a cytosolic invertase to negatively regulate sugar-mediated root growth. *Plant Cell*, **19**, 163-181.

Ma, H., Xu, S.P., Luo, D., Xu, Z.H. and Xue, H.W. (2004) OsPIPK 1, a rice phosphatidylinositol monophosphate kinase, regulates rice heading by modifying the expression of floral induction genes. *Plant Mol Biol*, **54**, 295-310.

Malhó, R. (2006) *The Pollen Tube: A Cellular and Molecular Perspective*.

McKinney, E.C., Kandasamy, M.K. and Meagher, R.B. (2001) Small changes in the regulation of one Arabidopsis profilin isovariant, PRF1, alter seedling development. *Plant Cell*, **13**, 1179-1191.

Menand, B., Calder, G. and Dolan, L. (2007) Both chloronemal and caulonemal cells expand by tip growth in the moss Physcomitrella patens. *J Exp Bot*, **58**, 1843-1849.

Mikami, K., Saavedra, L., Hiwatashi, Y., Uji, T., Hasebe, M. and Sommarin, M. (2010) A dibasic amino acid pair conserved in the activation loop directs plasma membrane localization and is necessary for activity of plant type I/II phosphatidylinositol phosphate kinase. *Plant Physiol*, **153**, 1004-1015.

Mueller-Roeber, B. and Pical, C. (2002) Inositol phospholipid metabolism in Arabidopsis. Characterized and putative isoforms of inositol phospholipid kinase and phosphoinositide-specific phospholipase C. *Plant Physiol*, **130**, 22-46.

Perroud, P.F. and Quatrano, R.S. (2006) The role of ARPC4 in tip growth and alignment of the polar axis in filaments of Physcomitrella patens. *Cell Motil Cytoskeleton*, **63**, 162-171.

Ramachandran, S., Christensen, H.E., Ishimaru, Y., Dong, C.H., Chao-Ming, W., Cleary, A.L. and Chua, N.H. (2000) Profilin plays a role in cell elongation, cell shape maintenance, and flowering in Arabidopsis. *Plant Physiol*, **124**, 1637-1647.

Rensing, S.A., Lang, D., Zimmer, A.D., Terry, A., Salamov, A., Shapiro, H., Nishiyama, T., Perroud, P.F., Lindquist, E.A., Kamisugi, Y., Tanahashi, T., Sakakibara, K., Fujita, T., Oishi, K., Shin, I.T., Kuroki, Y., Toyoda, A., Suzuki, Y., Hashimoto, S., Yamaguchi, K., Sugano, S., Kohara, Y., Fujiyama, A., Anterola, A., Aoki, S., Ashton, N., Barbazuk, W.B., Barker, E., Bennetzen, J.L., Blankenship, R., Cho, S.H., Dutcher, S.K., Estelle, M., Fawcett, J.A., Gundlach, H., Hanada, K., Heyl, A., Hicks, K.A., Hughes, J., Lohr, M., Mayer, K., Melkozernov, A., Murata, T., Nelson, D.R., Pils, B., Prigge, M., Reiss, B., Renner, T., Rombauts, S., Rushton, P.J., Sanderfoot, A., Schween, G., Shiu, S.H., Stueber, K., Theodoulou, F.L., Tu, H., Van de Peer, Y., Verrier, P.J., Waters, E., Wood, A., Yang, L., Cove, D., Cuming, A.C., Hasebe, M., Lucas, S., Mishler, B.D., Reski, R., Grigoriev, I.V., Quatrano, R.S. and Boore, J.L. (2008) The Physcomitrella genome reveals evolutionary insights into the conquest of land by plants. *Science*, **319**, 64-69.

Saavedra, L., Balbi, V., Dove, S.K., Hiwatashi, Y., Mikami, K. and Sommarin, M. (2009) Characterization of phosphatidylinositol phosphate kinases from the moss Physcomitrella patens: PpPIPK1 and PpPIPK2. *Plant Cell Physiol*, **50**, 595-609.

Schaefer, D.G. and Zryd, J.P. (1997) Efficient gene targeting in the moss Physcomitrella patens. *Plant Journal*, **11**, 1195-1206.

Schaefer, D.G. and Zryd, J.P. (2001) The moss Physcomitrella patens, now and then. *Plant Physiol*, **127**, 1430-1438.

Schumaker, K.S. and Dietrich, M.A. (1997) Programmed changes in form during moss development. *Plant Cell*, **9**, 1099-1107.

Sousa, E., Kost, B. and Malho, R. (2008) Arabidopsis phosphatidylinositol-4-monophosphate 5-kinase 4 regulates pollen tube growth and polarity by modulating membrane recycling. *Plant Cell*, **20**, 3050-3064.

Stenzel, I., Ischebeck, T., Konig, S., Holubowska, A., Sporysz, M., Hause, B. and Heilmann, I. (2008) The type B phosphatidylinositol-4-phosphate 5-kinase 3 is essential for root hair formation in Arabidopsis thaliana. *Plant Cell*, **20**, 124-141.

Thimann, K.V., Reese, K. and Nachmias, V.T. (1992) Actin and the elongation of plant cells. *Protoplasma*, **171**, 153-166.

Thole, J.M. and Nielsen, E. (2008) Phosphoinositides in plants: novel functions in membrane trafficking. *Curr Opin Plant Biol*, **11**, 620-631.

Vidali, L., Augustine, R.C., Kleinman, K.P. and Bezanilla, M. (2007) Profilin is essential for tip growth in the moss Physcomitrella patens. *Plant Cell*, **19**, 3705-3722.

Vincent, P., Chua, M., Nogue, F., Fairbrother, A., Mekeel, H., Xu, Y., Allen, N., Bibikova, T.N., Gilroy, S. and Bankaitis, V.A. (2005) A Sec14p-nodulin domain phosphatidylinositol transfer protein polarizes membrane growth of Arabidopsis thaliana root hairs. *J Cell Biol*, **168**, 801-812.

Yin, H.L. and Janmey, P.A. (2003) Phosphoinositide regulation of the actin cytoskeleton. *Annu Rev Physiol*, **65**, 761-789.

Short legends for Supporting Information

Supplemental figure 1. Scheme of the disruption of the *PpPIPK1* and *PpPIPK2* loci.

Supplemental figure 2. Disruption of the *PpPIPK1* and *PpPIPK2* in the HGT-1 line.

Supplemental figure 3. Effects of *pipk1* and *pipk2* mutations on the actin cytoskeleton in chloronemal cells.

Tables

Table 1. Primer sequences used in this study

PpPIPK1 genomic sequence	5'-AAGGCATCTGTATTTGACGAGGAC-3'
	5'-AATACACTCCACGACACTAAGAGAGACTC-3'
PpPIPK2 genomic sequence	5'-TTCTGGAGACCTCTTTGTGCGGTAGTG-3'
	5'-TCGATATTCTCTCCCACATTCTCTGACC-3'
PpPIPK1KO 5'g fragment	5'-CTAGGGTCGAACA<u>CTCGAG</u>AGGTTGTTG-3'
	5´-AGGGGTGC<u>GTCGAC</u>CCCAAGGC-3'
PpPIPK1KO 3'g fragment	5'-TGGGCTTTTACAGGT<u>ACTAGT</u>CTAAGCAG-3'

	5'-CTCACCAAAGTGTAAT<u>GGTACC</u>TTCCACAG-3'
PpPIPK2KO 5'g fragment	5'-GACACTT<u>AAGCTT</u>GGTTTCCGATCAGAC-3'
	5'-GTCAATTTTGCCC<u>CCGCGG</u>ACCTGCTGAT-3'
PpPIPK2KO 3'g fragment	5'-CTCTCC<u>GAGCTC</u>CTCTGACCAAGAATAGAT-3'
	5'- GAGGTGTTGCAAGTCATGTTTATCA-3'
PpPIPK1 RT-PCR fragment	5'- CTTGTATGCGTGCTCTATGCGTTTGCT -3'
	5'- TAGGTGGTGTTTCAAGCTGTGC-3'
PpPIPK2 RT-PCR fragment	5'- CTTGTATGCGTGCTCTATGCGTTTGCT -3'
	5'- TAGGTGGTGTTTCAAGCTGTGC-3'
Pp18S RT-PCR fragment	5'-TTGACTCAACACGGGGAAAC-3'
	5'-AGCTGATGACTCGCGCTTAC-3'
PpPIPK1 CDs	5'- CACC**ATG**TCTGAAGGGCTTTATG-3'
	5'- **TCA**TAGTTGGGTAGGAGGAAAAATCT-3'
PpPIPK2 CDs	5' - CACC**ATG**CGAAGTCCTGCTTCTA- 3'
	5' - TCATTCGTTCAAATGAGTTGGAGGA- 3'

FIGURE LEGENDS

Figure 1. **Comparison of the phenotype of *P. patens* wild type, and of the single and double *pipk* knockout mutants at different developmental stages.**

(A) Three-week-old colonies growing in 100X diluted minimal media, bar = 0.5 cm. (B) Three-week-old colonies growing in minimal media, bar = 0.5 cm. (C) Six-day-old protonema filaments growing on minimal media, bar = 200 μm. (D) Five-week-old leafy shoots, bar = 2.5 mm. (E) Sporophyte induction, bar = 1 mm. (F) Morphometric parameters of wild type and transformants. Total area values in cm^2 and solidity defined as area/convex hull area (plants with values approaching one are more compact) represented in the graphs.

Figure 2. The levels of PtdIns(4,5)*P$_2$* are reduced in *P. patens pipk* mutants. Phospholipids were extracted and separated by thin-layer-chromatography. The levels of PtdIns(4,5)P$_2$, PtdCho (phosphatidylcholine), PtdIns (phosphatidylinositol) from protonema tissue of wild type controls and the *pipk* lines grown under normal growth conditions were determined by quantifying the amount of associated fatty acids.. Data represent the means ± SE of four independent experiments. Bgr, background signal without sample.

Figure 3. The *P. patens pipk* mutants are impaired in caulonemal cell development.

(A) Chlorophyll a+b content in wild type and *pipk* transformants. (B) Values of average cell length in micrometers measured on subapical cells of wild type and transformant

31

protonemal cells growing in minimal media. (C) Wild type and *pipk* transformants were grown vertically in the dark for 20 days, bar = 0.5 cm.

Figure 4. The *P. patens pipk* mutants are impaired in rhizoid elongation.

(A) Twenty- day-old gametophores of wild type and *pipk* transformants, bar = 0.5 cm. (B) Values of average rhizoid lengths in centimetres.

Figure 5. Effects of the F-actin drugs Cyt B and Lat B on *P. patens* wild type and *pipk* mutants.

A) Protonemal tissue was treated for one week with 10 μM Cyt B or DMSO as control. Bar = 500 μm.

B) Five-day-old protoplasts from wild type and *pipk* mutants growing in media containing DMSO, 10 μM Cyt B or 5 μM of Lat B. Protoplasts were isolated and after two days of growth under normal conditions they were transferred to the indicated media. Pictures were taken after 5 or 7 days, respectively. Bar = 200 μm.

Figure 6. Comparison of the phenotype of *P. patens* wild type, *pipk1, pipk1+ PpPIPK1, pipk1-2 and pipk1-2+ PpPIPK2* knock out mutants at different developmental stages.

A) a) Three-week-old colonies growing in 100X diluted minimal media, bar = 0.5 cm. b) Three-week-old colonies growing in minimal media, bar = 0.5 cm. c) Six-day-old protonema filaments growing on minimal media, bar = 200 μm.

B) RT-PCR analysis of transformant and wild type using specific primers RT1f and RT1r for *PIPK1* or RT2f and RT2r for *PIPK2*. As an internal control, a 400 bp fragment of *Physcomitrella* 18S cDNA was used.

C) Values of average rhizoid lengths in centimetres of twenty-day-old gametophores of wild type and *pipk* transformants.

D) Values of average cell length in micrometers measured on subapical cells of wild type and transformants protonemal cells growing in minimal media.

Figure 7. **Effects of *pipk1* and *pipk2* mutations on the actin cytoskeleton** CLSM images of six-day-old protonema of *hgt-1* (A, D), *pipk1 (hgt-1)* (B, E) and *pipk2* (*hgt-1*) (C, F) strains overproducing GFP-talin. A, B, C are apical caulonemal cells and D, E, F are subapical caulonemal cells. Asterisks indicate the caulonemal cell wall. Arrows in A, B and C, indicate the F-actin cap array located either at the end of the tip or at its apical side. The bar with arrow seen in panel A indicates the apicobasal gradient of the cortical actin meshwork observed in caulonemal cells. A-F bar = 20 μm.

Supplemental Figure 1. **Scheme of the disruption of the *PpPIPK1* and *PpPIPK2* loci.**
(A) Schematic representation of the genomic locus of *PpPIPK1* and *PpPIPK2*, and the derived constructs used in this study for the disruption of the *PpPIPK* locus by homologous recombination. White and grey boxes correspond to exons and introns, respectively. The locations of the primers used (in B and C) are shown by arrowheads. (B) PCR genotyping analysis of the transformants and the wild type. Gene targeting events were detected by

simultaneous PCR amplifications utilizing gene-specific primers external to the targeting construct (PL1 and PR1 or PL2 and PR2 for *PIPIK1* and *PIPK2*, respectively) in combination with outward-pointing primers specific to the selectable marker cassette (P35S and PnptII for *PIPK1* and PcamVR and PnptII3 for *PIPK2*). Left border, LB; right border, RB. (C) RT-PCR analysis of transformants and wild type using specific primers RT1f and RT1r for *PIPK1* or RT2f and RT2r for *PIPK2*. As an internal control, a 400 bp fragment of *Physcomitrella* 18S cDNA was used.

Supplemental figure 2. Disruption of the *PpPIPK1* and *PpPIPK2* in the HGT-1 line.

A) (a) Three-week-old colonies growing in minimal media, bar = 0.5 cm, (b) Three-week-old colonies growing in 100X diluted minimal media, bar = 0.5 cm, (c) Six-day-old protonema filaments growing on minimal media, bar = 200 μm. B) RT-PCR analysis of *pipk* transformants and the HGT-1 line using specific primers as described in Figure 1. As an internal control, a 400 bp fragment of *Physcomitrella* 18S cDNA was used. C) PCR genotyping analysis of *pipk* transformants and the HGT-1 line using specific primers as described in Figure 1. Gene targeting events were detected by simultaneous PCR amplifications utilizing gene-specific primers external to the targeting construct in combination with outward-pointing primers specific to the selectable marker cassette. Left border, LB; right border, RB. D) Values of average cell length in micrometers measured on subapical cells of HGT-1 line and *pipk* transformant protonemal cells growing in minimal media. E) Values of average rhizoid lengths in centimetres of twenty-day-old gametophores of HGT-1 and *pipk* transformants.

Supplemental figure 3. **Effects of *pipk1* and *pipk2* mutations on the actin cytoskeleton in chloronemal cells.** CLSM images of six-day-old chloronemal cells of *hgt-1* (A), *pipk1 (hgt-1)* (B) and *pipk2* (*hgt-1*) (C) strains overproducing GFP-talin. Arrows indicate the F-actin cap array located at the end of the tip. A-C bar = 10 μm.
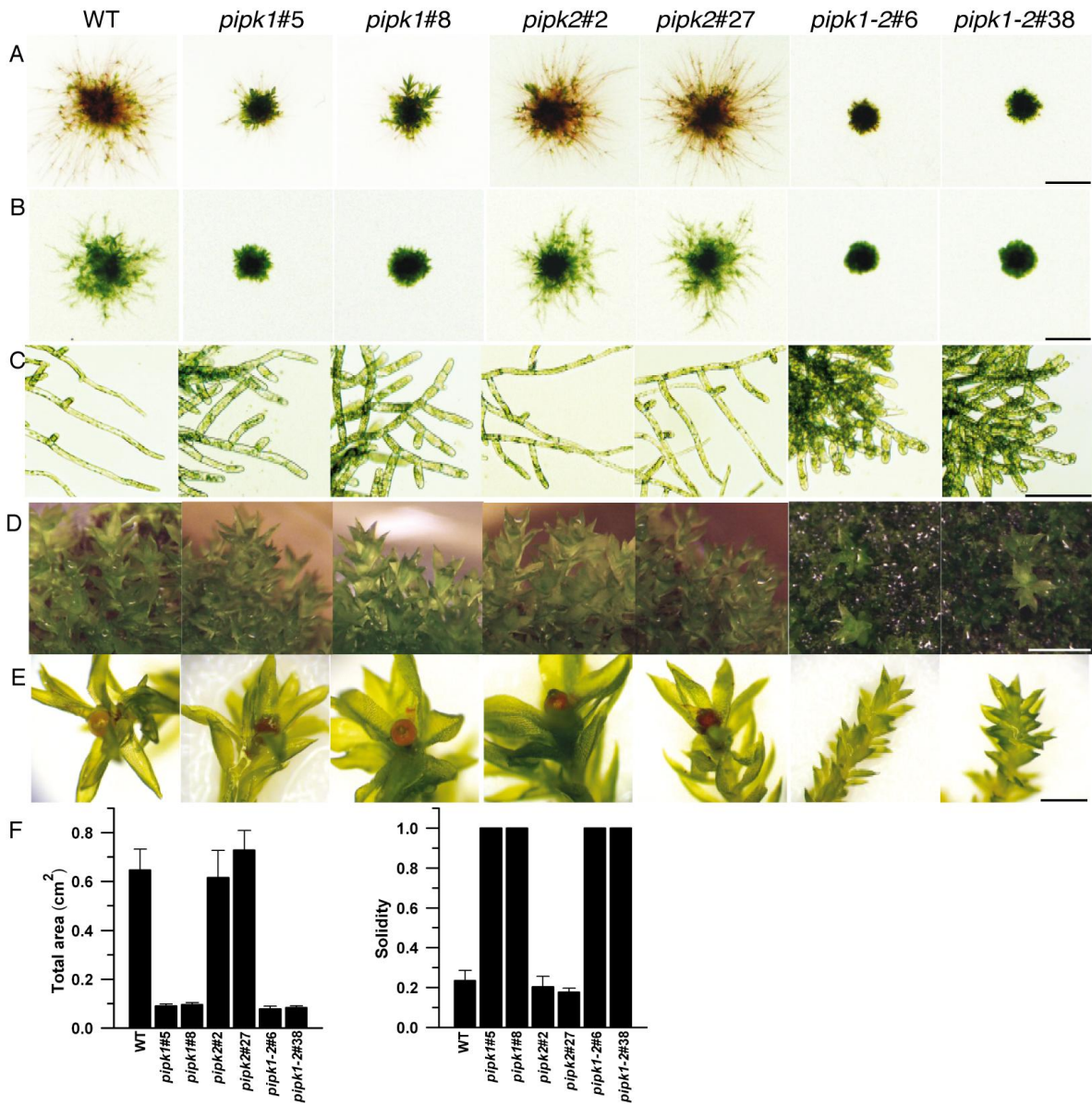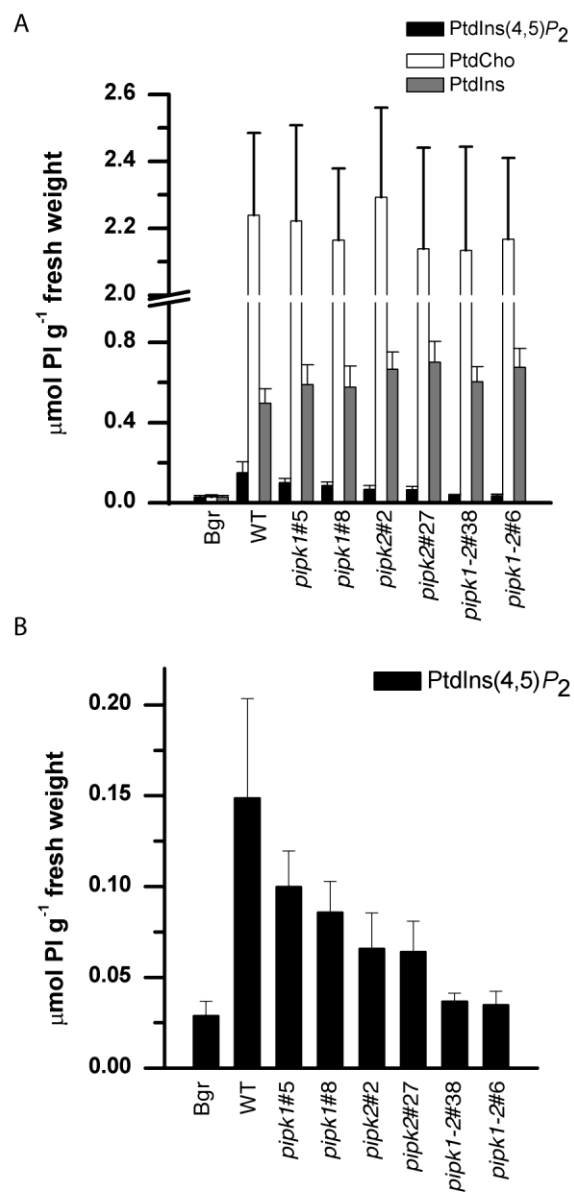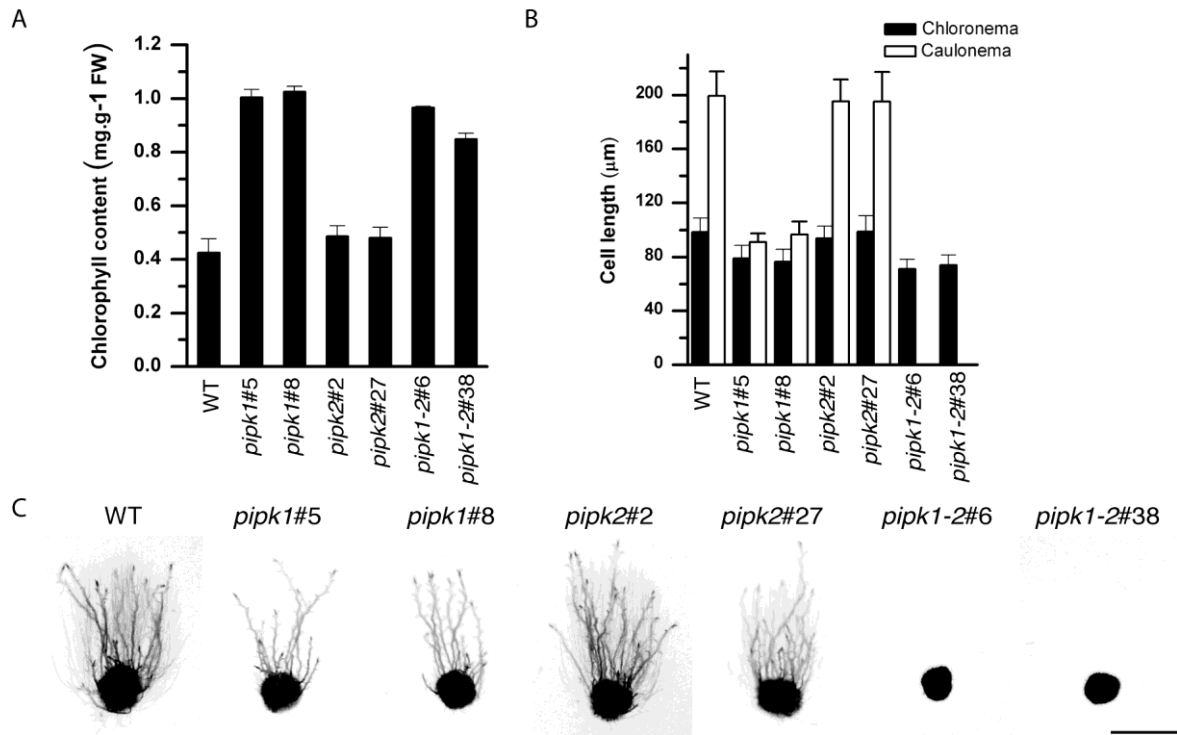
Figure 1

Figure 2

Figure 3

Figure 4

Figure 5

Figure 6

A

| | WT | *pipk1#8* | *pipk1#8 +*
PpPIPK1 | *pipk1#8 +*
PpPIPK1E885A | *pipk1-2#38* | *pipk1-2#38 +*
PpPIPK2 |

a)

b)

c)

B

PpPIPK1

PpPIPK2

Pp18S

WT
pipk1#8
pipk1#8 + PpPIPK1#16
pipk1#8 + PpPIPK1E885A#13
pipk1-2#38
pipk1-2#38 + PpPIPK2#1

C

Rhizoid length (cm)

WT
pipk1#8
pipk1#8 + PpPIPK1#16
pipk1#8 + PpPIPK1E885A#13
pipk1-2#38
pipk1-2#38 + PpPIPK2#1

D

Cell length (μm)

Chloronema
Caulonema

WT
pipk1#8
pipk1#8 + PpPIPK1#16
pipk1#8 + PpPIPK1E885A#13
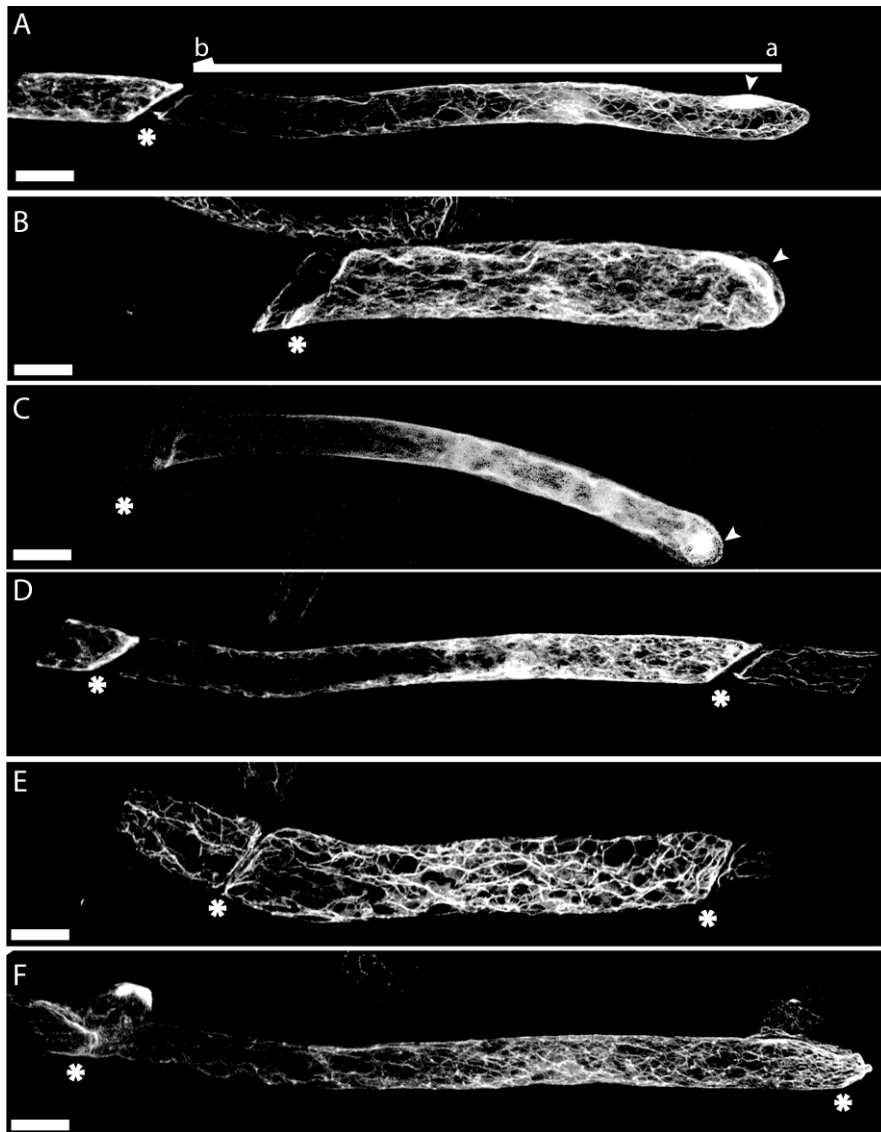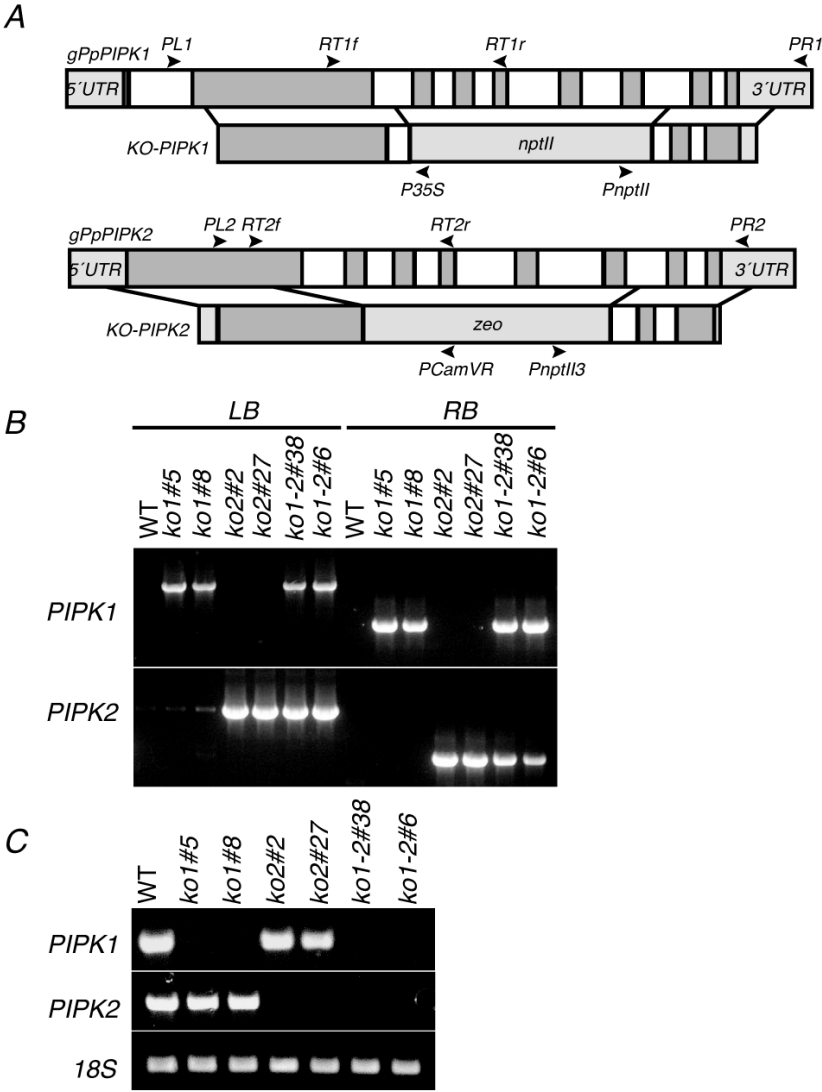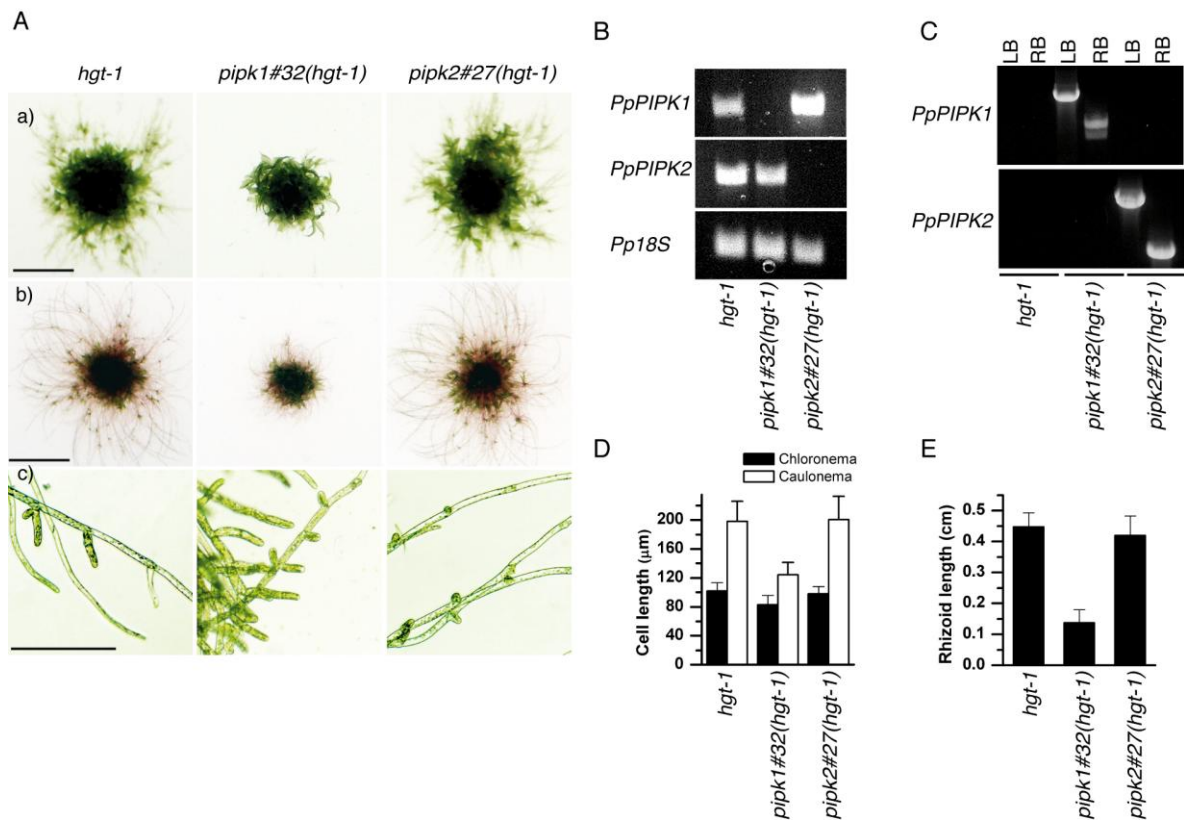*pipk1-2#38*
pipk1-2#38 + PpPIPK2#1

41

Figure 7

Supplemental Figure 1

Supplemental Figure 2

Supplemental Figure 3